MODEL TEST ON THE AXIAL CAPACITY OF DISPLACEMENT RIBBED PILES

Abideen Adekunle Ganiyu[a]*, Ahmad Safuan A. Rashid[a], Mohd Hanim Osman[b]

[a]Department of Geotechnics and Transportation, Faculty of Civil Engineering, Universiti Teknologi Malaysia, 81310 UTM Johor Bahru, Johor, Malaysia
[b]Forensic Engineering Centre, Institute for Smart Infrastructure and Innovative Construction, Faculty of Civil Engineering, Universiti Teknologi Malaysia, 81310 UTM Johor Bahru, Johor, Malaysia

Graphical abstract

Abstract

The capacity, hence the load-settlement behaviour of a pile is governed by the collective behaviour of the base and shaft. It is highly desirable, sustainable and economical to accommodate the increasing demand for deeper and wider foundations through the use of higher capacity piles. This research investigated the performance of preformed displacement ribbed piles in a unit gravity model test. Four tests were carried out to replicate the constant rate of penetration (CRP) test in the field. Two lengths corresponding to short and long piles for each of plain and ribbed piles were employed. Compacted Kaolin S300 type was employed as the model soil. The failure load of the piles was determined using six different methods. An increased capacity of 32% and 20% was obtained in the short and long ribbed piles, respectively. Also, it was observed that the closer the distance between the ribs, the higher the capacity produced for equal number of ribs. The ribbed piles gave higher capacities through the increase in their shaft capacity which is associated with the presence of ribs along their lengths. An increase in the axial capacity of displacement piles can be attained by modifying the profile of the pile shaft through the use of ribs.

Keywords: Ribbed piles; model test; failure load; pile capacity

Abstrak

Kapasiti, tingkah laku beban-enapan diambil kira oleh tingkah laku kolektif asas dan aci. Ia adalah sangat wajar, merujuk kepada keadaan ekonomi dan keboleupayaan untuk mempertahankan sumber asal untuk menampung permintaan yang semakin meningkat untuk asas-asas yang lebih dalam dan lebih luas melalui penggunaan cerucuk yang berkapasiti lebih tinggi. Kajian ini menyiasat prestasi cerucuk anjakan berusuk pra-bentuk dalam ujian model unit graviti. Empat ujian telah dijalankan mewakili ujian kadar penembusan malar (CRP) di lapangan. Dua cerucuk yang berbeza panjang mewakili cerucuk pendek dan panjang telah digunakan. Tanah Kaolin S300 terpadat telah digunakan sebagai model tanah. Kegagalan beban cerucuk ditentukan dengan menggunakan enam kaedah yang berbeza. Kapasiti meningkat sebanyak 32% dan 20% telah diperolehi masing-masing untuk cerucuk berusuk pendek dan panjang. Selain itu, diperhatikan juga ledih dekat rusuk maka lebih kapasiti diperolehi bagi jumlah rusuk yang sama. Cerucuk berusuk memberikan kapasiti yang lebih tinggi melalui peningkatan kapasiti aci yang dikaitkan dengan kehadiran rusuk di sepanjang aci. Peningkatan dalam kapasiti paksi cerucuk anjakan boleh dicapai dengan mengubah profil aci cerucuk dengan menggunakan tulang rusuk.

Keywords: Cerucuk berusuk; model ujian; beban gagal; kapasiti cerucuk

1.0 INTRODUCTION

Piles are utilised to transmit loadings from superstructures through weak or compressible strata or water to a firmer soil or rock layer. They are needed to prevent settlements, resist axial, lateral, cyclic and uplift loads [1, 2]. The capacity, hence the load-settlement behaviour of a pile is governed by the collective behaviour of the base and shaft. Ideally, the shaft capacity is mobilised at much smaller displacements than the base capacity [3, 4]. The shaft resistance develops at a relatively small settlements about 0.5% of the shaft diameter, whereas the base resistance needs a larger resistance of about 10-20% of the base diameter to fully develop [4]. The pile shaft resistance is influenced by the state and properties of soils within the critical zone immediately surrounding the pile; the method used for driving the pile; the roughness of the pile surface (i.e., pile materials); and the state of the pile end. The longer the pile, the larger the contribution of the pile shaft resistance to the axial load carried by the pile [5, 6].

In recent times, there is an increasing need to construct taller structures in more confined spaces or on weaker soils; this leads to demands for deeper and wider pile foundations[7]. However, it is more desirable to produce piles of higher capacity to accommodate this demand. In addition to being cost-effective, this is highly sustainable based on the reduced consumption of concrete, lower excavations and lesser spoil removal; which eventually leads to a green environment. Ribbed piles have been shown to have enhanced shaft capacity when compared with the conventional plain (straight shafted) piles. Rib designs such as concentric, helical, tapered and under reamed ribs have been experimented at various spacing and different outstand, thickness and distance between the ribs for bored cast in-situ piles [8-10].

The capacity of piles are commonly verified through full scale axial compression load tests[11]. The pile head load-movement comprises three components viz; the load-movement of the pile toe, the elastic compression of the pile and the load-movement of the shaft resistance. The relative magnitude of the three dictates the load-displacement response of a pile while the shaft resistance exhibits the ultimate resistance[12]. However, full scale tests are costly to undertake [13-15], hence physical modelling are increasingly being used to study geotechnical engineering systems [16, 17]. Bearing capacity of a pile is conventionally defined as the load corresponding to a settlement equal to 10% of pile diameter [18, 19]. Other common criteria for load test interpretation are discussed in [20-22].

In a bid to broaden the usability of ribbed piles, this research examines the performance of displacement ribbed piles in a unit gravity model test using Kaolin soil. Four model tests were carried out to replicate the constant rate of penetration (CRP) test in the field. Two lengths corresponding to short and long piles for each of plain and ribbed piles were employed respectively.

2.0 METHODOLOGY

2.1 Materials

a) Kaolin – The model soil used is the commercially manufactured powdered kaolin S300 type supplied by Kaolin (Malaysia) Sdn. Bhd. Kaolin is chemically known as hydrated Aluminium Silicate. It is structurally unmodified, platy in structure, hydrophilic, readily water dispersible with a pH range between 3.5 and 6.0 and loss on ignition of 2-6% at 1025^OC. Table 1 shows the chemical composition of this product obtained by XRF method as supplied by the manufacturer [23]. Functionally, the model soil is to provide penetration resistance to the model pile along its entire shaft and base. The choice of a manufactured clay is premised on its ability to lessen variability and enhance repeatability of the results.

Table1 Chemical composition of Kaolin S300 type

Element	Oxide Formula	Composition
Aluminium	Al_2O_3	7-12%
Silica	SiO_2	80-90%
Iron	Fe_2O_3	<1%
Potassium	K_2O	<2%
Magnesium	MgO	<0.5%

b) Model Piles: Four stainless steel circular moulds, two each of lengths 100 mm and 150 mm were fabricated. The diameter of the moulds are 24 mm. The lengths are for short and long piles based on Brom's classification (l/d < 5 and l/d > 5 accordingly). Additionally, to ensure comparison between the ribbed piles, equal number (5) inverted-vee-shaped dents of 2 mm depth of width and length 10 mm and 6 mm (anterior and posterior) respectively at equal spacing of 18 mm and 27 mm (short and long piles respectively) were made inside two of the moulds to create corrugations during casting (Figure 1). The model piles were cast with mortar in the laboratory according to BS EN 998-2 [24]. A mix ratio of 1:3 for cement: sand and a water: cement ratio of 0.45 was used, the casting was demoulded after 24

hours and cured in water for 28 days. The corrugations later translated to ribs after setting and demoulding the piles (Figures 2 and 3).
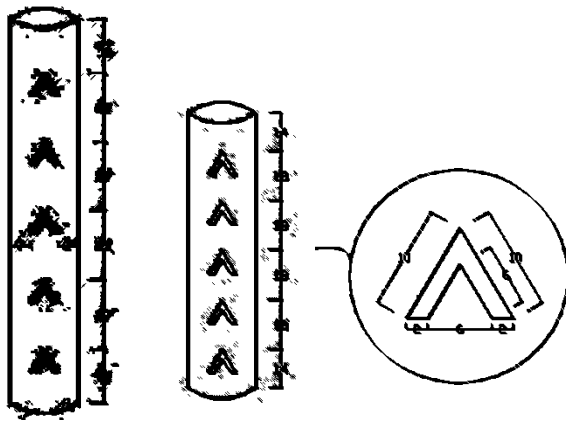

Figure 1 Moulds for ribbed piles

Figure 2 A schematic diagram of the ribbed piles showing the dimensions and the details of the rib

Figure 3 Long and short, plain and for ribbed piles

2.2 Testing Equipment

a) Testing chamber: This is a rigid box having dimensions (320 x 150 x 430) mm length, width and height, respectively. The front face of the chamber is a removable 20 mm thick rigid Perspex panel which facilitates real time view of the testing while the remaining three sides are made from Aluminium panels. All the sides were fixed tightly using 'M8' bolts which prevented lateral movements. Four steel rods 20 mm in diameter were located beside the testing chamber; they were attached to a base plate and were used to mount the loading frame. The loading plates and the base plate are made of Aluminium with dimensions (660 x 300 x 20) mm length, width and thickness, respectively.

b) Driving unit: The driving unit was fixed on the loading plate. The drive shaft is made from a solid stainless steel rod and a stopper was installed inside the drive shaft to prevent the rod from rotating during the displacement process. A two way motor was used to rotate the central drive shaft via a rubber belt. A Panasonic 825 Watt speed controller was connected to the motor as a power source. The controller has variable speed control and a two way switch which could change the movement of the shaft either upwards or downwards (Figure 4).

c) Transducers and Data Acquisition System: A 25 mm stroke length Linear Variable Displacement Transducer (LVDT) was utilised for measuring the displacement of the model piles during the loading stage. A 2.0 kN load cell transducer was utilised to measure the force during the loading. The LVDT was connected to the CR800 data logging device and the input signals were recorded on a computer connected to the data logger. A logging software "Loggernet 4.0" was installed on the desktop and utilised for the data acquisition (Load Cell and LVDT).

Other tools employed include a wooden hammer (100 x 60 x 200)mm head, (40 x 20 x 300)mm handle weighing 1.17 kg; 2 porous plastics(320 x 150 x 5) mm; spatulas; mixing tray (600 x 600 x 60)mm; hand trowels and wash bottles.

2.3 Preparation of Soil Model

For each test, 14 kg of Kaolin clay was weighed in the mixing tray. 2.1 kg of water was intermittently added and the sample was thoroughly mixed using hand trowels until a uniform consistency was attained. A porous plastic was placed at the bottom of the testing chamber to prevent soil particles from leaking from the testing chamber, then the sample was added in 5 layers of comparable mass, each layer was compacted with 25 blows of hammer. The spatula was utilised to create uneven surface in between the layers. The second porous plastic was placed over the final compacted soil layer to ensure a flat surface. A

hole of 24 mm in diameter was made at the centre of the porous plastic and this was marked as the position for the installation of the pile. The porous plastic was then removed and the model pile was driven through the marked position into the soil to reach the same level with the top of the soil model.

2.4 Load Test

During the pile load test, the load cell and the round tipped adaptor were mounted at the end of the drive shaft and carefully lowered until the adaptor tip came into contact with the top of the pile. The LVDT was mounted on the top of the driving shaft by attaching it to a retort stand to measure the settlement of the pile. The load and settlement of the pile during the test were recorded by the logging system. The tests were ended when the penetration of the pile reached approximately 20 mm depth, a point at which the pile must have failed based on all available failure calculation methods. The undrained strength and moisture content of the soil were determined prior to the loading test. A 20 x 40 mm hand held vane tester was employed for the strength test while the moisture content test was done according to BS 1377-2:1990:3.2. The process was repeated for each of the model piles.

2.5 Failure Load Determination Methods

The following interpretation methods for load tests were employed in this research to obtain the measured capacities (Q_m) of the piles.
  i   10% of pile diameter settlement [18, 19, 21].
  ii   15% of pile diameter settlement [20].
  iii 6 mm settlement [21].
  iv   DeBeer (1970) [26, 27]: It is the load at the change in slope on a log-log load settlement curve, obtained at the intersection of two line approximations connecting the data at before and after the failure load.
  v   Chin (1970) [26, 27]: It is the inverse slope (1/m) of a line s/p = ms+c, where p = load and s = total settlement, obtained by dividing each settlement by its corresponding load and plotting the resulting value against the settlement.
  vi   Hansen 80 % (1963) [26, 28, 29]: A plot of the square root of settlement divided by its load value against the settlement was made. The ultimate load equals {1/ (2√C1C2) where C1 and C2 are the slope and intercept of the plot.

Figure 4 Set-up for the load tests

2.6 Predicted Capacity of Model Piles

The static formula is the basic approach to the design of piles based on Soil Mechanics principles [25]; it was employed to compute the predicted capacity (Q_P) of the piles (Equation 1).

$$Q_{ult} = A_b (c_u N_c) + (\alpha c_u) A_s \qquad [1]$$

Where Q_{ult} =ultimate pile capacity; A_b = base area; A_s =shaft area; N_c = bearing capacity factor; c_u = undrained shear strength and α = adhesion factor. The adhesion factor α is "the ratio of skin friction mobilised on the pile shaft to the undrained shear strength of the undisturbed clay" [9]. In this research, α = 1- 0.0011(c_u -25) for $25 \leq c_u \leq 70$ was adopted [1], N_c was taken as 9 and a factor of safety (FOS) of 2 was adopted, Q_P (design load) = Q_{ult} / FOS.

3.0 RESULTS AND DISCUSSION

3.1 Properties of Kaolin

To obtain the particle size distribution of the kaolin type S300, both the dry sieving and the hydrometer tests were carried out according to BS 1377-2: 1990:9.2 and 9.5, respectively. The result revealed that most of the soil particles (99.3 %) fall between 0.001 – 0.212 mm in size and the clay is a well-graded soil. The particle size distribution curve is shown in Figure 5. Atterberg limits tests were carried out according to BS 1377-2: 1990:5.3 and 4.3, the liquid limit obtained is 37 % while the plastic limit is 28 %, this implies that the plasticity index is 9 %. These results are in conformity with the values obtained by Marto *et.al* [30-32] for the same type of Kaolin.   The specific gravity of the clay from the small pycnometer test carried out according to BS 1377-2: 1990:8.3 is 2.65. Based on AASHTO classification system, Kaolin S300 is a low plasticity silt and falls in

Group A-4 while it is classified as ML based on USCS classification. Kaolin soil classified as ML but termed as clay has also been used by other previous researchers [33-35].

The moisture content of the soil model was designed to be 15 % and this was confirmed from the result of the moisture contents test carried out on the sample. The dry density of the clay was 1.38 Mg/m³, while the bulk density obtained was 1.59 Mg/m³ at 15 % moisture content. Also, the average undrained shear strength c_u of the soil model was 60 kPa. The soil model is a stiff soil based on the value of c_u obtained. The properties of the soil were consistent for all the four models.
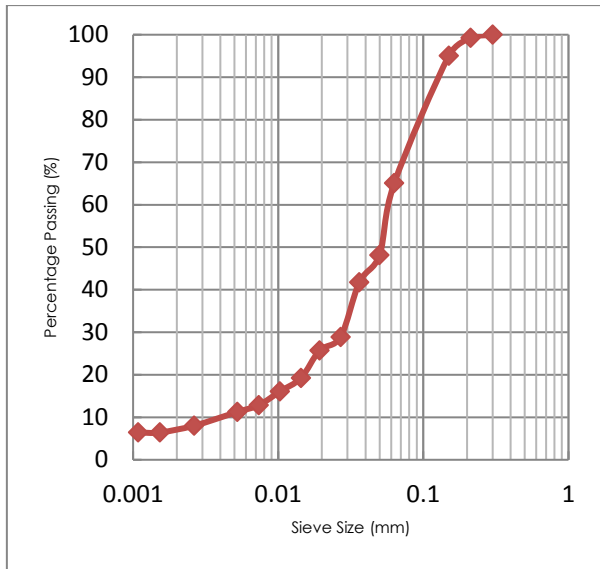

Figure 6 Load-displacement plot for the load tests

Figure 5 Particle size distribution curve for Kaolin S300

Figure 7 Load-displacement plot based on De-Beer (1970) method

3.2 Capacity of Piles

Figure 6 is the load- settlement plot for the four tests while Figures 7-9 show the graphs based on the methods (iv-vi) i.e. DeBeer (1970), Chin (1970) and Hansen 80 % (1963), respectively. Table 2 shows the measured capacity (Q_m) based on the selected failure load interpretation methods.

By comparing the average Q_m for the long piles (PP2 & RP2), an increase of 19.5 % was observed for the long piles while an increase of 32.1 % was observed for the short piles (PP1 & RP1). These imply that ribs accounted for these increases, the increase is more prominent in the short pile because the number of ribs per unit length of the pile is higher when compared with the long pile based on the spacing of the ribs.
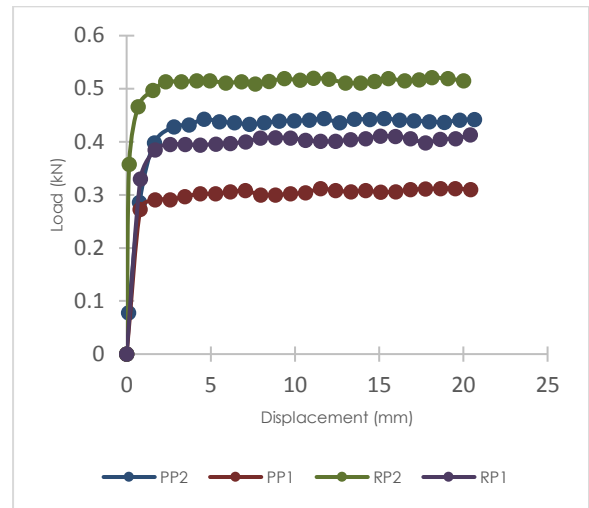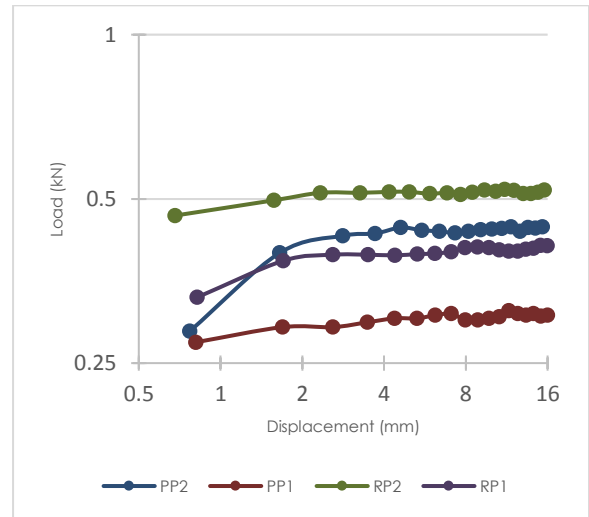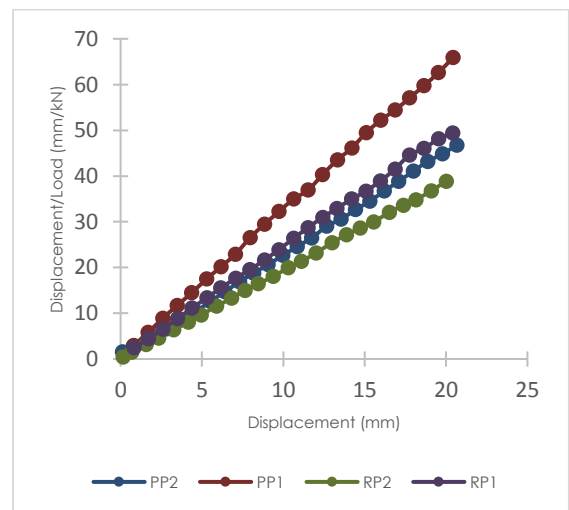

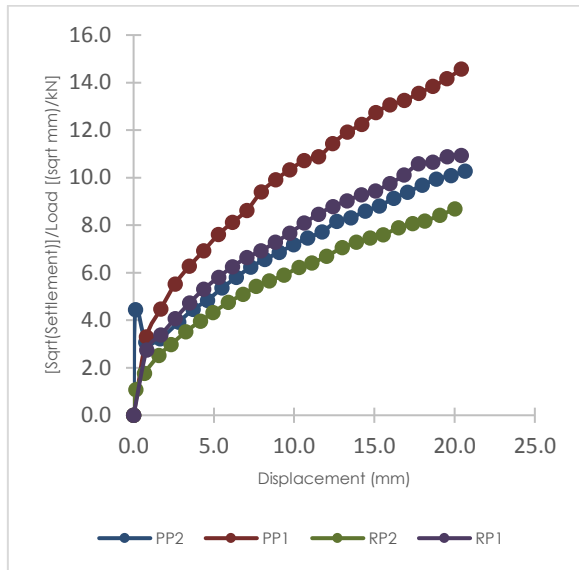**Figure 8** Load-displacement plot based on Chin (1970) method

Figure 9: Load-displacement plot based on Hansen 80% (1963) method

The predicted capacity (Q_P) of the piles were 0.448 kN & 0.340 kN for the long and short piles, respectively. This implies that the average Q_m for the model piles was lower for the plain piles by 1.8 % and 9.4 % for the long piles while it is higher by 17.4 % and 19.7 % in the ribbed piles. The ribs accounted for these differences in the capacity of the piles.

From back-calculations, it was observed that the shaft resistance of the ribbed piles at the failure load was higher than that of the plain piles. The shaft capacity for the long ribbed pile was 76.8 % as compared to 72.5 % of the plain long pile. Also the shaft capacity was 70.0 % to 60.4 % for the ribbed and plain short piles respectively. Again, the difference was higher in the short pile which has a closer arrangement of the ribs.

The ribbed piles gave higher capacities through the increase in their shaft capacity. This is distinctively associated with the presence of ribs (corrugations) along their lengths. The corrugations caused an increase in the skin friction, hence a higher adhesion factor α for the ribbed pile.

Table 2 Failure loads (kN) of the piles from different interpretation methods and the average values

	$Q_{m(10\% of diameter)}$	$Q_{m(15\% of diameter)}$	$Q_{m(6mm settlement)}$	$Q_{m(DeBeer)}$	$Q_{m(Chin)}$	$Q_{m(Hansen)}$	$Q_{m(Av.)}$
PP2	0.420	0.432	0.436	0.436	0.447	0.470	0.440
RP2	0.512	0.516	0.512	0.514	0.519	0.585	0.526
PP1	0.292	0.296	0.304	0.304	0.313	0.337	0.308
RP1	0.392	0.396	0.396	0.401	0.410	0.444	0.407

PP1= Plain pile 100 mm long; PP2= Plain pile 150 mm long; RP1= Ribbed pile 100 mm long and RP2 = Ribbed pile 150 mm long

4.0 CONCLUSION

This research employed unit gravity model test to examine the influence of ribs on the ultimate capacity of displacement piles. The use of model test in this study relieved the use of the usual full scale test which is highly expensive to execute. Prior researches on ribbed piles focused on cast-in-situ bored piles while this research extend it to preformed displacement piles. Five unique inverted-vee-shaped dents were employed to form the ribs on the model piles. Compacted kaolin clay was used to model stiff clay in the laboratory.

The load test results revealed that ribbed piles have higher capacity when compared with plain piles of equal dimensions. A significant increase of 32.1% was observed in the short pile because of the closer rib spacing employed. The ribs increased the shaft resistance of the ribbed pile via an increased skin friction in the piles. It is obvious from this research that an increased axial capacity of displacement piles can be attained by modifying the profile of the pile shaft. This can be done by using ribbed displacement piles.

Acknowledgement

References

[1]   Viggiani, C., Mandolini, A. and Russo, G. 2012. *Piles and Pile Foundation*. London: Spon Press.
[2]   Momeni, E., Nazir, R., Armaghani, D. J., and Maizir. H. 2014. Prediction of Pile Bearing Capacity Using A Hybrid Genetic Algorithm-Based ANN. *Measurement*, 57:122-131.
[3]   Bell, A., and Robinson, C. 2012. Single Piles, in Manual of Geotechnical Engineering. Institution of Civil Engineers: United Kingdom: 803-821.
[4]   Burland, J. B. 2012. Behaviour of Single Piles under Vertical Loads, in Manual of Geotechnical Engineering. Institution of Civil Engineers: United Kingdom: 231-246.
[5]   Helal, A. A. 2012. *Axially Loaded Pile Behavior in Sands With/Without Limited Liquefaction, in Department of Civil and Environmental Engineering*. The University of Alabama in Huntsville: Huntsville, Alabama.
[6]   Fleming, K., Weltman, A., M. Randolph and K. Elson. 2009. *Piling Engineering*. 3rd ed. London: Taylor & Francis.

[7]   Doherty, P., and Gavin, K. 2011. The Shaft Capacity of Displacement Piles in Clay: A State of the Art Review. *Geotechnical and Geological Engineering*, 29(4): 389-410.

[8]   Witton-Dauris, J. B. 2012. Centrifuge Modelling of High Shear Capacity Ribbed Piles in Stiff Clay. Geotechnical Engineering Research Group. City University London: London: 171.

[9]   Gorasia, R. J. 2013. *Behaviour of Rbbed Piles in Clay*. Doctoral dissertation, City University.

[10]   Gorasia, R. J. and McNamara, A.M. 2012. High Shear Capacity Ribbed Piles. In *Eurofuge 2012, Delft, The Netherlands, April 23-24, 2012*. Delft University of Technology and Deltares.

[11]   Nazir, R., Moayedi, H., Mosallanezhad, M. and Tourtiz, A. 2015. Appraisal of Reliable Skin Friction Variation in A Bored Pile. *Proceedings of the Institution of Civil Engineers-Geotechnical Engineering*, 168(1):75-86.

[12]   Fellenius, B.H. 2001. We Have Determined the Capacity, Then What. *Deep Foundation Institute, Fulcrum*: 23-26.

[13]   Hajialilue-Bonab, M., Levacher, D., Chazelas, J.L. and Kaynia, A.M. 2014. Experimental Study on the Dynamic Behavior of Laterally Loaded Single Pile. *Soil Dynamics and Earthquake Engineering*, 66: 157-166.

[14]   Sakr, M. 2013. Comparison Between High Strain Dynamic And Static Load Tests Of Helical Piles In Cohesive Soils. *Soil Dynamics and Earthquake Engineering*. 54: 20-30.

[15]   Momeni, E., Maizir, H., Gofar, N. and Nazir, R. 2013. Comparative Study on Prediction of Axial Bearing Capacity of Driven Piles in Granular Materials. *Jurnal Teknologi*, 61(3): 15-20.

[16]   Ong, D.E.-L., Leung, C.F., and Chow, Y. K. 2005. The Role of Physical Modelling to Study Geotechnical Failures. *3rd International Young Geotechnical Engineer Conference*. Osaka, Japan.

[17]   Kim, N.-R. and Kim, D. S. 2011. The Role of Physical Modeling in the Design of Geotechnical Systems. *First International Workshop on Design in Civil and Environmental Engineering*. KAIST:11-18.

[18]   Jabatan Kerja Raya Malaysia. 2005. *JKR 20800 2005* Standard Specification for Building Works. Malaysia.

[19]   British Standards Institution. 2014. *Eurocode 7:* Geotechnical Design Part 1: General Rules.

[20]   Institution of Civil Engineers. 2007. I*CE Specification for Piling and Embedded Retaining Walls.* 2nd edition ed. London: Thomas Telford Publishing,.

[21]   Tomlinson, M. and J. Woodward. 2014. *Pile Design and Construction Practice*. 6th ed. CRC Press.

[22]   [22] Fellenius, B.H. 1999. *Basics of Foundation Design*. Richmond, BC: BiTech Publishers Limited.

[23]   Kaolin (Malaysia) Sdn Bhd. 2014. Kaolin Clay (S300) *Technical data sheet*.

[24]   British Standards Institution. 2013. *Specification for Mortar for Masonry Part 2: Masonry Mortar*. BSI Standards Publication.

[25]   Dithinde, M., Phoon, K.K., De Wet, M. and Retief, J.V. 2010. Characterization of Model Uncertainty in the Static Pile Design Formula. *Journal of Geotechnical and Geoenvironmental Engineering*. 137(1): 70-85.

[26]   Fellenius, B.H. 2001. *What Capacity Value to Choose from the Results of A Static Loading Test*. Deep Foundation Institute. Fulcrum.

[27]   Marcos, M.C.M., Chen, Y.J and Kulhawy, F.H. 2013. Evaluation of Compression Load Test Interpretation Criteria for Driven Precast Concrete Pile Capacity. *KSCE Journal of Civil Engineering*. 17(5): 1008-1022.

[28]   [Paikowsky, S.G. and Tolosko, T.A. 1999. Extrapolation of Pile Capacity from Non-Failed Load Tests.

[29]   Ng, C.W.W., Yau, T.L.Y., Li, J. H. M. and Tang, W.H. 2001. New Failure Load Criterion for Large Diameter Bored Piles in Weathered Geomaterials. *Journal of Geotechnical and Geoenvironmental Engineering*. 127(6): 488-498.

[30]   Marto, A., Abdullah, M. H., Rosly, N. A., Aziz, N. and Rahman, N. A. A. 2014. Maximizing the Use of Coal Ash in Soft Soil Improvement. *National Geofest*. 2014, UTHM, Batu Pahat, Malaysia.

[31]   Marto, A., Hasan, M., Hyodo, M., and Makhtar, A.M. 2014. Shear Strength Parameters and Consolidation of Clay Reinforced with Single and Group Bottom Ash Columns. *Arabian Journal for Science and Engineering*, 39(4): 2641-2654.

[32]   Marto, A., Makhtar, A.M., and Amaludin, A. 2015. Comparisons on the Response Of Shallow Geothermal Energy Pile Embedded In Soft And Firm Soils, *Jurnal Teknologi*, 77(11): 137-143)

[33]   Stewart, M.A. and McCartney, J.S. 2014. Centrifuge Modeling of Soil-Structure Interaction in Energy Foundations. *Journal of Geotechnical and Geoenvironmental Engineering*, 140(4): 1-11.

[34]   Kavak, A. and G. Baykal. 2011. Long-Term Behavior of Lime-Stabilized Kaolinite Clay. *Environmental Earth Sciences*. 66(7): 1943-1955.

[35]   Stewart, M.A. and J.S. McCartney. 2012. Strain Distributions in Centrifuge Model Energy Foundations. *ASCE GeoCongress. Oakland, California*.